

RESEARCH ARTICLE

Open Access



Precipitation of manganese oxides on the surface of construction materials in the Khmer temples, Cambodia

Etsuo Uchida^{1*}, Ryota Watanabe¹ and Satomi Osawa²

Abstract

Background: In addition to the blackening caused by blue-green algae growth, other black areas on the surface of construction materials (e.g., sandstone, laterite and bricks) are frequently observed in the Khmer temples in Cambodia. A non-destructive on-site investigation was carried out using a portable X-ray fluorescence analyzer (pXRF). In addition, samples were taken from the buildings and were analyzed using an X-ray diffractometer (XRD) and a scanning electron microscope with an energy dispersive X-ray spectrometer, and were observed using a field emission scanning electron microscope.

Results and conclusions: A non-destructive investigation using the pXRF revealed that this blackening was caused by manganese oxide precipitates. The precipitates contained small amounts of Ni, V, Zn, Y, K, Cl, S, Pb, and Cr. The XRD analysis indicated that the manganese oxides were mainly present as an amorphous phase, but some formed birnessite and todorokite. The manganese precipitates were mostly in a hexagonal plate form (100–300 nm), but some were in a rod-shape, which may have been caused by the activity of manganese oxidizing microbes. Preliminary experiments on removal of manganese oxide precipitates were conducted. The manganese oxide precipitates could be easily removed using a reducing agent such as an oxalic acid solution.

Keywords: Manganese oxide, Manganese oxidizing microbe, Birnessite, Todorokite, Khmer temple, Cambodia

Background

Sandstone, laterite and bricks were the major construction materials used by the Khmer people in their temples, including the Angkor monuments in Cambodia during the ninth to fifteenth centuries [1, 2]. With the passage of time, the surfaces of these materials have blackened. Most of this discoloring is caused by blue-green algae (cyanobacteria), which gradually damage the bas-relief carvings on these temples [3]. In addition, black areas with more luster than the blue-green algae are frequently observed on the surface of the construction materials in the Khmer temples. Similar blackening has been also observed on the surface of Mesopotamian clay tablets, and analysis indicated that this was caused by manganese

oxide precipitates [4]. This is similar to desert varnish, which contains manganese and iron oxides and is found on stone surfaces in the desert [5–7]. To date, no study has been conducted to investigate if the blackening on the Khmer temples is caused by manganese oxide precipitates. Although this black material does not seem to damage the construction materials, it has changed the color of the temples so they no longer appear as they did in their original condition. To prevent further blackening, this study aimed to determine if the blackening on the surface of construction materials in the Khmer temples is caused by precipitation of manganese oxides, and also to elucidate the precipitation mechanism.

A non-destructive on-site investigation was carried out using a portable X-ray fluorescence analyzer (pXRF). In addition, samples were taken from the buildings and analyzed using an X-ray diffractometer (XRD) and a scanning electron microscope with an energy-dispersive

*Correspondence: weuchida@waseda.jp

¹ Department of Resources and Environmental Engineering, Waseda University, Ohkubo 3-4-1, Shinjuku-ku, Tokyo 169-8555, Japan
Full list of author information is available at the end of the article

X-ray spectrometer (SEM-EDX), and examined using a field emission scanning electron microscope (FE-SEM).

Methods

Sample site

The investigation was carried out at the Angkor, Koh Ker and Sambor Prei Kuk monuments in Cambodia, which were selected as sites that were representative of the Khmer monuments (Fig. 1). The Angkor monuments are located 250 km northwest of Phnom Penh, the capital of Cambodia. They were constructed during the ninth to fifteenth centuries. The Koh Ker monuments are located 85 km northeast of the Angkor monuments. This site was the capital of the Khmer empire from 921 to 944 AD. The Sambor Prei Kuk monuments are located 140 km south-east of the Angkor monuments, and construction at this site occurred in the pre-Angkorian period. The Sambor Prei Kuk monuments were the capital in the seventh century.

Blackening, suspected to be from manganese oxide precipitates, is observed on the surface of all types of construction materials used in the Khmer temples, including sandstone (feldspathic sandstone and siliceous

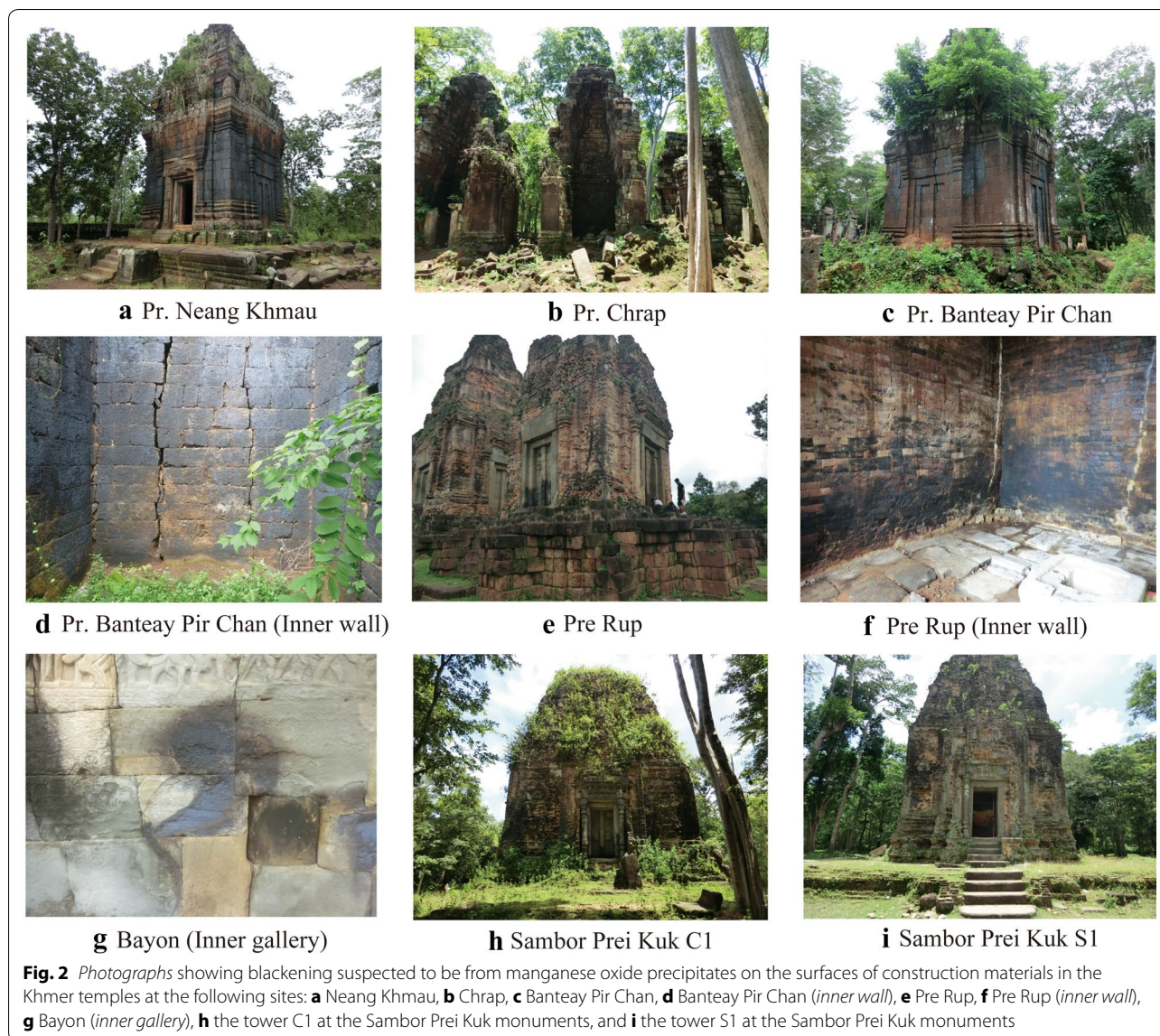
sandstone), laterite, and bricks. This discoloration is extensive on the surface of laterite at the Koh Ker monuments, especially on the Neang Khmau (Fig. 2a), Chrap (Fig. 2b), and Banteay Pir Chan (Fig. 2c, d) temples. Blackening is also evident on the surfaces of bricks and sandstone used in the southern brick towers situated on the eastern side of the Pre Rup temple at the Angkor monuments (Fig. 2e, f). Also at the Angkor monuments, there is blackening on the east side of the north face of the inner gallery of the Bayon temple (Fig. 2g). At the Sambor Prei Kuk monuments, there are black areas on the walls of the towers C1 (Fig. 2h) and S1 (Fig. 2i). Black areas are observed on both the inner and outer surfaces of the buildings (Fig. 2d, f). In addition to these sites, blackening is frequently observed at other Khmer architectural sites.

Analytical methods

The black materials, which were thought to be manganese oxide precipitates, were analyzed non-destructively on-site using a pXRF analyzer (Delta Premium, Innov-X Systems, Waltham, MA, USA) with an X-ray tube with a Rh target (4 W). The analysis was conducted in a soil mode



Fig. 1 Map showing the locations of the Angkor, Koh Ker, and Sambor Prei Kuk monuments in Cambodia



for 60 s at each point. Before analysis, the pXRF analyzer was calibrated for Mn, Ni, V, Zn, K, Pb, Cr, Sr, Cu, Ti, Rb, Ca, Fe and Zr using 10 rock standards obtained from the Geological Survey of Japan [8]. However the analysis for the black materials may be semi-quantitative because the black materials are as thin as less than 0.2 mm and X-ray penetrates into the under layer such as sandstone, laterite and bricks. Analyses were conducted on the blackened areas of the construction materials and also on non-blackened areas of the construction materials as controls. Five points were analyzed at each building, and the average values were calculated.

Construction materials covered with black materials were also taken from the buildings (sample nos. 3401–3414 in Table 1). The samples were taken from different

places, which were analyzed using the pXRF analyzer. The black materials on the surface of the samples were removed using a drill. The samples of the black materials were analyzed using an XRD (RINT-RAPID, Rigaku, Tokyo, Japan) with an X-ray tube with a Cu target. The current and voltage were 30 mA and 40 kV, respectively. Each scan was conducted from $2\theta = 2^\circ\text{--}60^\circ$ with a scan speed of $1^\circ/\text{min}$.

The black materials were also analyzed using a SEM-EDX (JSM6360, JEOL, Tokyo, Japan equipped with Inca Energy, Oxford Instruments, Abingdon, UK). The SEM-EDX analysis was conducted on a polished cross section of each sample. Samples for the SEM-EDX were first embedded in an epoxy resin (EpoFix, Struers, Ballerup, Denmark), and then polished with waterproof SiC paper (#180,

Table 1 List of the samples of black materials taken from the Khmer temples

Sample no.	Base material	Temple	Sampling point
3401	Sandstone	Bayon	East side of the north face of the inner gallery
3402	Laterite	Prasat Neang Khmau	Outer wall of the central tower
3403	Laterite	Prasat Chrap	Inner wall of the southern tower
3404	Laterite	Prasat Banteay Pir Chan	Inner wall of the central tower
3405	Laterite	East Mebon	Northwestern library
3406	Laterite	Pre Rup	Outer wall of the inner enclosure
3407	Sandstone	Pre Rup	Outer wall of the southernmost tower in the east towers
3408	Laterite	Ta Keo	Second platform
3409	Laterite	Phnom Krom	Outer wall of the enclosure
3410	Laterite	Wat Athvea	Inner wall of the enclosure
3411	Bricks	Sambor Prei Kuk	Outer wall of the tower S1
3412	Sandstone	Sambor Prei Kuk	Outer wall of the tower S1
3413	Bricks	Sambor Prei Kuk	Outer wall of the tower C1
3414	Sandstone	Sambor Prei Kuk	Outer wall of the tower C1

#800, #1200, and #2400 μm , Struers) and diamond paste (3 μm , Struers). Finally, the samples were coated with carbon. The accelerating voltage was 15 kV, and the beam current was adjusted so that the X-ray count was 2000 count/s on the Co surface. The measurement time was 60 s.

In addition, the surface of each black material sample was examined using a FE-SEM (4500S, Hitachi, Tokyo, Japan). The accelerating voltage was 15 kV, and the sample surface was coated with platinum-palladium ($\text{Pt}_{80}\text{Pd}_{20}$).

Results and discussion

pXRF analysis

Because the pXRF analysis was conducted in the air and in a soil mode, light elements such as Na, Mg, Al and Si which are major components of rocks, could not be analyzed. The pXRF results for the average chemical compositions at each building are summarized in Table 2. The ratio of each element in the black area to that in the non-black area is shown in Fig. 3. This shows that Mn was highly concentrated in the black areas (22,700–247,000 mg/kg) compared to the non-black areas. In addition, Ni, V, Zn, Y, K, Cl, S, Pb, and Cr were also concentrated in the black areas compared with the non-black areas. The average V content range was 1000–10,800 mg/kg, except for the tower C1 (sandstone) at the Sambor Prei Kuk monuments. The Ni content was high at the Koh Ker monuments (1400–2800 mg/kg). The Zn and Cr contents were high at the tower S1 at the Sambor Prei Kuk monuments, with concentrations of 2400 mg/kg (Zn) and 6000 mg/kg (Cr) recorded on bricks and 850 mg/kg (Zn) and 3600 mg/kg (Cr) on sandstone. The Fe content in the black areas was similar to that in the non-black areas. The

Mn content is generally less than 0.3 % in sandstone, laterite, and bricks [1, 2]. However, laterite at the Koh Ker monuments contains more Mn (0.3–2.4 %) [9]. This may be one of the reasons why precipitation of manganese oxides is remarkable on the surface of laterite at the Koh Ker monuments.

The enrichment of Mn, Ni, V, Zn, Y, Pb, and Cr in ferromanganese crusts against seawater was reported by Hein et al. [10]. In addition, the enrichment of K, Ni, Zn and Pb in rock varnish was reported by Dorn et al. [11]. The enrichment of Cl and S in the manganese oxides on the surface of the construction materials in the Khmer monuments may be attributable to bat guano [12].

SEM-EDX analysis

The black materials obtained from the different sites were less than 0.2 mm thick, but in some cases as thick as 0.5 mm (Fig. 4). The results from chemical analyses of these samples by the SEM-EDX are summarized in Table 3. In addition, SEM and X-ray images in the cross section of sample no. 3405 from the inner wall of East Mebon were shown in Fig. 4. The dominant element in the black areas was Mn, with a range of 4–48 %. Compared with the non-black areas, Mn was 10–390 times more concentrated in the black areas. The Al, Si, and Fe content ranges in the black areas were 3–19, 3–34, and 2–52 %, respectively. These elements could be attributed to the construction materials. P is distributed just on the surface of construction materials and is covered by black materials (Fig. 4). P is considered to have been derived from bat excrement. Trace elements detected by the pXRF such as Ni, V, Zn, Y, Pb, and Cr were not detected by the SEM-EDX because these elements were contained

Table 2 pXRF results for the black materials on the surface of the construction materials used in the Khmer temples

Temple	Mn ± s.d. (mg/kg)	Ni ± s.d. (mg/kg)	V ± s.d. (mg/kg)	Zn ± s.d. (mg/kg)	Y ± s.d. (mg/kg)	K ± s.d. (mg/kg)	Cl ± s.d. (mg/kg)
Bayon							
Blackened area	51,500 ± 28,800	156 ± 52	1030 ± 551	454 ± 188	57 ± 24	16,600 ± 4500	260 ± 155
Sandstone	297 ± 63	<6	378 ± 392	33 ± 9	16 ± 2	17,500 ± 2230	366 ± 181
Ratio	173.4	-	2.7	13.7	3.5	0.9	0.7
East Mebon							
Blackened area	93,900 ± 21,400	560 ± 289	4570 ± 1090	111 ± 63	72 ± 134	7650 ± 2920	1840 ± 503
Laterite	3185 ± 817	<18	3090 ± 1250	42 ± 49	43 ± 124	1910 ± 1700	613 ± 120
Ratio	29.5	-	1.5	2.6	1.7	4.0	3.0
Pre Rup							
Blackened area	81,100 ± 53,500	522 ± 359	3820 ± 1520	92 ± 48	128 ± 141	8400 ± 7130	523 ± 103
Laterite	2171 ± 2270	<26	1908 ± 738	42 ± 15	26 ± 11	6750 ± 7490	995 ± 476
Ratio	37.4	-	2.0	2.2	5.0	1.2	0.5
Blackened area	47,400 ± 12,600	85 ± 43	2530 ± 1750	41 ± 8	173 ± 142	10,200 ± 3890	3560 ± 1030
Sandstone	474 ± 119	<8	276 ± 358	33 ± 8	29 ± 19	16,600 ± 2400	1030 ± 532
Ratio	99.9	10.7	9.2	1.3	6.1	0.6	3.5
Blackened area	137,000 ± 61,400	123 ± 42	2660 ± 1360	593 ± 278	475 ± 153	18,700 ± 7790	10,500 ± 3530
Bricks	339 ± 102	17 ± 7	202 ± 126	15 ± 3	17 ± 8	1890 ± 174	1270 ± 883
Ratio	404.0	7.3	13.2	40.1	28.3	9.9	8.3
Ta Keo							
Blackened area	93,900 ± 33,400	560 ± 238	4570 ± 2440	111 ± 36	72 ± 57	7650 ± 5130	1840 ± 1930
Laterite	3185 ± 1701	<28	3090 ± 1450	42 ± 6	43 ± 28	1910 ± 1400	<613
Ratio	29.5	-	1.5	2.6	1.7	4.0	3.0
Phnom Krom							
Blackened area	188,000 ± 53,600	925 ± 350	2130 ± 2300	300 ± 76	30 ± 11	18,400 ± 5090	<469
Laterite	3130 ± 1670	<31	1216 ± 255	163 ± 54	14 ± 5	2700 ± 1900	424 ± 115
Ratio	41.5	-	3.9	1.7	2.4	4.2	2.8
Wat Athvea							
Blackened area	74,900 ± 16,700	247 ± 109	2300 ± 915	187 ± 121	445 ± 370	5100 ± 2460	1210 ± 531
Laterite	682 ± 399	<13	573 ± 174	73 ± 31	103 ± 54	2250 ± 632	507 ± 291
Ratio	110.0	-	4.0	2.6	4.3	2.3	2.4
Pr. Neang Khmau							
Blackened area	146,000 ± 73,000	1480 ± 804	4800 ± 1220	27 ± 98	116 ± 80	16,900 ± 20,400	<629
Laterite	12,700 ± 1340	<34	1842 ± 661	46 ± 9	17 ± 10	2420 ± 820	833 ± 148
Ratio	20.0	-	2.6	2.0	7.2	12.6	1.4
Pi. Chrap							

Table 2 continued

Temple	Mn ± s.d. (mg/kg)	Ni ± s.d. (mg/kg)	V ± s.d. (mg/kg)	Zn ± s.d. (mg/kg)	Y ± s.d. (mg/kg)	K ± s.d. (mg/kg)	Cl ± s.d. (mg/kg)
Blackened area	214,000 ± 129,000	2750 ± 1700	3180 ± 1390	453 ± 348	498 ± 332	9890 ± 5900	2530 ± 1370
Laterite	3670 ± 1040	<40	1800 ± 308	83 ± 68	49 ± 44	4020 ± 2510	1130 ± 273
Ratio	58.3	-	1.8	5.4	10.2	2.5	2.2
Pr. Banteay Pir Chan							
Blackened area	248,000 ± 68,600	2320 ± 707	3740 ± 1430	99 ± 66	197 ± 81	24,500 ± 17,200	<629
Laterite	24,000 ± 20,300	103 ± 76	2770 ± 515	89 ± 21	48 ± 28	3330 ± 1720	1000 ± 142
Ratio	10.3	22.5	1.3	1.1	4.1	7.3	-
Sambor Prei Kuk Tower S1							
Blackened area	22,700 ± 8170	178 ± 156	10,800 ± 6150	2420 ± 2560	648 ± 494	5660 ± 3660	1190 ± 312
Bricks	460 ± 180	10 ± 4	142 ± 84	35 ± 7	31 ± 8	5100 ± 1370	279 ± 43
Ratio	49.4	18.8	76.4	68.7	21.0	1.1	4.3
Blackened area	79,500 ± 44,400	182 ± 143	7740 ± 2620	846 ± 728	338 ± 195	16,000 ± 3940	1580 ± 1130
Sandstone	572 ± 365	<14	132 ± 100	38 ± 9	22 ± 12	19,100 ± 1990	343 ± 196
Ratio	139.0	13.0	58.5	22.5	15.5	0.8	4.6
Sambor Prei Kuk Tower C1							
Blackened area	188,000 ± 178,000	47 ± 28	1650 ± 1300	103 ± 54	85 ± 105	28,400 ± 24,900	2940 ± 2840
Bricks	1012 ± 756	13 ± 12	150 ± 82	53 ± 31	31 ± 8	6750 ± 4750	823 ± 681
Ratio	186.0	3.7	11.0	1.9	2.7	4.2	3.6
Blackened area	39,200 ± 18,000	32 ± 15	181 ± 62	30 ± 4	17 ± 1	16,900 ± 2130	6910 ± 4300
Sandstone	463 ± 45	<7	129 ± 32	42 ± 9	22 ± 2	22,500 ± 1880	1030 ± 184
Ratio	84.5	4.5	1.4	0.7	0.8	0.8	6.7
Temple	S ± s.d. (mg/kg)	Pb ± s.d. (mg/kg)	Cr ± s.d. (mg/kg)	Co ± s.d. (mg/kg)	Sr ± s.d. (mg/kg)	P ± s.d. (mg/kg)	As ± s.d. (mg/kg)
Bayon							
Blackened area	1540 ± 618	40 ± 19	398 ± 318	5 ± 4	215 ± 18	2730 ± 1170	7 ± 3
Sandstone	5450 ± 7380	16 ± 4	64 ± 22	12 ± 1	220 ± 6	<2270	4 ± 2
Ratio	0.3	2.5	6.2	0.4	1.0	1.2	1.8
East Mebon							
Blackened area	5510 ± 2270	67 ± 27	1270 ± 308	155 ± 23	121 ± 297	5020 ± 6050	62 ± 174
Laterite	2890 ± 4180	38 ± 133	1500 ± 570	254 ± 73	70 ± 461	16,500 ± 3690	55 ± 241
Ratio	1.9	1.8	0.8	0.6	1.7	0.3	1.1
Pre Rup							
Blackened area	3760 ± 1180	80 ± 85	987 ± 695	323 ± 100	140 ± 117	5220 ± 911	55 ± 37
Laterite	2530 ± 1020	25 ± 7	654 ± 533	289 ± 92	69 ± 44	8870 ± 2860	56 ± 76
Ratio	1.5	3.1	1.5	1.1	2.0	0.6	1.0
Blackened area	3050 ± 670	35 ± 13	1400 ± 1030	<2	241 ± 80	5220 ± 2000	7 ± 1

Table 2 continued

Temple	S ± s.d. (mg/kg)	Pb ± s.d. (mg/kg)	Cr ± s.d. (mg/kg)	Co ± s.d. (mg/kg)	Sr ± s.d. (mg/kg)	P ± s.d. (mg/kg)	As ± s.d. (mg/kg)
Sandstone	863 ± 502	8 ± 1	172 ± 219	13 ± 3	194 ± 21	3630 ± 2400	<2
Ratio	3.5	4.4	8.1		1.2	1.4	-
Blackened area	7110 ± 5030	40 ± 26	1350 ± 743	19 ± 15	66 ± 23	31,600 ± 21,500	<3
Bricks	1810 ± 746	9 ± 5	79 ± 44	<1	30 ± 8	3940 ± 1850	<3
Ratio	3.9	4.2	17.2	14.5	2.2	8.0	-
Ta Keo							
Blackened area	5510 ± 1900	67 ± 66	1270 ± 619	155 ± 23	121 ± 40	5020 ± 1300	62 ± 27
Laterite	2890 ± 1290	38 ± 18	1510 ± 942	254 ± 53	70 ± 26	16,500 ± 5930	55 ± 24
Ratio	1.9	1.8	0.8	0.6	1.7	0.3	1.1
Phnom Krom							
Blackened area	3400 ± 4900	126 ± 41	660 ± 873	214 ± 45	51 ± 18	31,300 ± 16,300	93 ± 30
Laterite	2760 ± 1950	76 ± 50	362 ± 257	298 ± 83	44 ± 12	57,400 ± 35,700	76 ± 23
Ratio	2.6	1.2	4.6	0.7	1.2	0.5	1.2
Wat Athvea							
Blackened area	6773 ± 9340	157 ± 82	944 ± 534	<11	229 ± 29	8660 ± 7590	148 ± 67
Laterite	7440 ± 12,900	48 ± 23	210 ± 63	180 ± 103	190 ± 22	3850 ± 1200	163 ± 53
Ratio	0.9	3.3	4.5	0.1	1.2	2.2	0.9
Pr. Neang Khmau							
Blackened area	<1720	<10	2340 ± 569	<15	134 ± 35	14,700 ± 5170	12 ± 4
Laterite	4070 ± 1160	<14	1470 ± 332	150 ± 63	85 ± 32	19,100 ± 10,900	18 ± 7
Ratio	1.3	-	1.0	-	1.6	0.8	0.7
Pr. Chirap							
Blackened area	6230 ± 1720	<21	701 ± 423	207 ± 127	515 ± 153	25,000 ± 9050	13 ± 5
Laterite	7620 ± 3290	<14	2000 ± 1080	192 ± 78	307 ± 269	18,200 ± 6960	32 ± 11
Ratio	0.8	-	0.3	1.1	1.7	1.4	0.4
Pr. Banteay Pir Chan							
Blackened area	1620 ± 97	<10	917 ± 302	<16	424 ± 116	23,400 ± 5720	14 ± 6
Laterite	4100 ± 1190	<10	2280 ± 791	121 ± 68	582 ± 312	25,900 ± 7720	28 ± 14
Ratio	0.4	-	0.4	-	0.7	0.9	0.5
Sambor Prei Kuk Tower S1							
Blackened area	21,200 ± 25,187	31 ± 20	6000 ± 3510	29 ± 12	73 ± 24	16,200 ± 11,300	9 ± 5
Bricks	1737 ± 1423	18 ± 6	69 ± 35	3 ± 1	38 ± 6	<3330	5 ± 0
Ratio	12.2	1.7	87.3	9.4	1.9	4.8	1.8
Blackened area	10,890 ± 7470	48 ± 51	3600 ± 1930	35 ± 23	314 ± 120	13,000 ± 10,600	15 ± 14
Sandstone	6590 ± 11,300	16 ± 8	55 ± 16	9 ± 2	248 ± 15	<1140	<2
Ratio	1.7	2.9	65.3	4.1	1.3	-	7.7

Table 2 continued

Temple	S ± s.d. (mg/kg)	Pb ± s.d. (mg/kg)	Cr ± s.d. (mg/kg)	Co ± s.d. (mg/kg)	Sr ± s.d. (mg/kg)	P ± s.d. (mg/kg)	As ± s.d. (mg/kg)
Sambor Prei Kuk Tower C1							
Blackened area	3790 ± 2360	14 ± 7	541 ± 476	<2	369 ± 598	<2860	5 ± 2
Bricks	947 ± 544	16 ± 6	56 ± 18	5 ± 2	60 ± 18	<1250	10 ± 2
Ratio	4.0	0.8	9.7	-	6.2	-	0.6
Blackened area	4940 ± 1970	14 ± 2	56 ± 8	<2	244 ± 8	<4390	<2
Sandstone	681 ± 271	12 ± 1	77 ± 11	14 ± 2	240 ± 5	<1550	<4
Ratio	7.3	1.2	0.7	0.1	1.0	2.8	-
Temple	Cu ± s.d. (mg/kg)	Ti ± s.d. (mg/kg)	Rb ± s.d. (mg/kg)	Ca ± s.d. (mg/kg)	Mo ± s.d. (mg/kg)	Fe ± s.d. (mg/kg)	Zr ± s.d. (mg/kg)
Bayon							
Blackened area	13 ± 4	2780 ± 597	56 ± 5	11,600 ± 2720	<2	17,100 ± 1480	114 ± 27
Sandstone	13 ± 5	2630 ± 928	62 ± 3	20,300 ± 8410	<2	15,800 ± 2150	127 ± 27
Ratio	1.0	1.1	0.9	0.6	-	1.1	0.9
East Mebon							
Blackened area	87 ± 22	13,400 ± 1220	21 ± 5	14,100 ± 1950	7 ± 2	355,000 ± 274,000	167 ± 48
Laterite	117 ± 15	11,600 ± 3180	13 ± 6	16,000 ± 1320	6 ± 2	430,000 ± 191,000	195 ± 33
Ratio	0.7	1.2	1.7	0.9	1.2	0.8	0.9
Pre Rup							
Blackened area	105 ± 163	10,400 ± 2580	21 ± 10	11,320 ± 4120	8 ± 3	292,000 ± 172,000	145 ± 25
Laterite	130 ± 78	9180 ± 2970	15 ± 5	9710 ± 2250	6 ± 3	333,000 ± 113,000	126 ± 41
Ratio	0.8	1.1	1.3	1.2	1.3	0.9	1.2
Blackened area	40 ± 16	4670 ± 928	58 ± 7	10,700 ± 958	3 ± 0	19,300 ± 2250	181 ± 10
Sandstone	15 ± 3	2830 ± 492	68 ± 9	9900 ± 346	3 ± 1	18,200 ± 2300	227 ± 62
Ratio	2.7	1.6	0.8	1.1	1.0	1.1	0.8
Blackened area	45 ± 9	3390 ± 467	15 ± 6	20,100 ± 4510	3 ± 1	8400 ± 1010	193 ± 23
Bricks	16 ± 4	2860 ± 332	14 ± 3	8130 ± 476	3 ± 1	9960 ± 1870	201 ± 23
Ratio	2.8	1.2	1.1	2.5	0.8	0.8	1.0
Ta Keo							
Blackened area	87 ± 26	13,400 ± 3560	21 ± 7	14,100 ± 1200	7 ± 3	355,000 ± 132,000	167 ± 32
Laterite	117 ± 37	11,600 ± 2470	13 ± 2	16,000 ± 6960	6 ± 3	430,000 ± 144,000	195 ± 29
Ratio	0.7	1.2	1.7	0.9	1.2	0.8	0.9
Phnom Krom							
Blackened area	45 ± 16	8220 ± 1920	13 ± 7	9070 ± 1360	5 ± 2	309,000 ± 76,200	110 ± 10
Laterite	83 ± 4	5400 ± 1100	22 ± 12	9750 ± 1590	5 ± 1	209,000 ± 90,500	113 ± 29
Ratio	0.5	1.5	0.6	0.9	1.1	1.5	1.0
Wat Athvea							
Blackened area	75 ± 22	6830 ± 2260	20 ± 13	11,200 ± 3490	7 ± 1	124,000 ± 100,000	127 ± 29

Table 2 continued

Temple	Cu ± s.d. (mg/kg)	Ti ± s.d. (mg/kg)	Rb ± s.d. (mg/kg)	Ca ± s.d. (mg/kg)	Mo ± s.d. (mg/kg)	Fe ± s.d. (mg/kg)	Zr ± s.d. (mg/kg)
Laterite	76 ± 15	3760 ± 721	20 ± 5	14,500 ± 7200	7 ± 2	93,000 ± 51,900	120 ± 30
Ratio	1.0	1.8	1.0	0.8	1.0	1.3	1.1
Pr. Neang Khmau							
Blackened area	<16	19,700 ± 2490	9 ± 1	7785 ± 1420	8 ± 1	403,000 ± 48,000	173 ± 17
Laterite	52 ± 35	20,800 ± 3680	<7	31,900 ± 9600	7 ± 1	529,000 ± 36,300	208 ± 22
Ratio	-	0.9	1.3	0.2	1.1	0.8	0.8
Pr. Chirap							
Blackened area	161 ± 85	13,900 ± 4650	12 ± 2	8750 ± 2430	10 ± 5	193,000 ± 51,000	179 ± 54
Laterite	59 ± 45	26,300 ± 8040	-	13,200 ± 4320	14 ± 8	656,000 ± 127,000	199 ± 39
Ratio	2.7	0.5	-	0.7	0.7	0.3	0.9
Pr. Banteay Pir Chan							
Blackened area	<15	23,500 ± 4640	12 ± 4	7990 ± 2130	10 ± 4	402,000 ± 59,700	216 ± 30
Laterite	46 ± 20	33,800 ± 4100	6 ± 2	13,300 ± 3780	22 ± 12	681,000 ± 161,000	194 ± 41
Ratio	-	0.7	2.0	0.6	0.5	0.6	1.1
Sambor Prei Kuk Tower S1							
Blackened area	54 ± 29	6370 ± 2470	57 ± 18	13,400 ± 9070	3 ± 1	9220 ± 444	273 ± 23
Bricks	16 ± 2	2760 ± 263	60 ± 9	8480 ± 1930	4 ± 2	10,400 ± 346	279 ± 32
Ratio	3.3	2.3	1.0	1.6	0.8	0.9	1.0
Blackened area	37 ± 19	6800 ± 3650	74 ± 13	13,700 ± 4680	4 ± 1	13,500 ± 1790	136 ± 93
Sandstone	13 ± 2	1950 ± 286	67 ± 2	21,100 ± 16,100	21 ± 26	18,700 ± 2890	276 ± 357
Ratio	2.9	3.5	1.1	0.6	0.2	0.7	0.5
Sambor Prei Kuk Tower C1							
Blackened area	32 ± 21	3690 ± 1510	58 ± 18	23,300 ± 16,100	9 ± 4	8500 ± 1650	225 ± 86
Bricks	22 ± 5	2750 ± 282	70 ± 13	8000 ± 1310	5 ± 1	10,500 ± 810	277 ± 65
Ratio	1.4	1.3	0.8	2.9	2.0	0.8	0.8
Blackened area	8 ± 3	198 ± 178	67 ± 3	19,700 ± 4430	3 ± 1	16,600 ± 629	142 ± 21
Sandstone	22 ± 13	3150 ± 208	93 ± 10	11,100 ± 453	3 ± 1	25,200 ± 1220	253 ± 84
Ratio	0.4	0.6	0.7	1.8	0.8	0.7	0.6

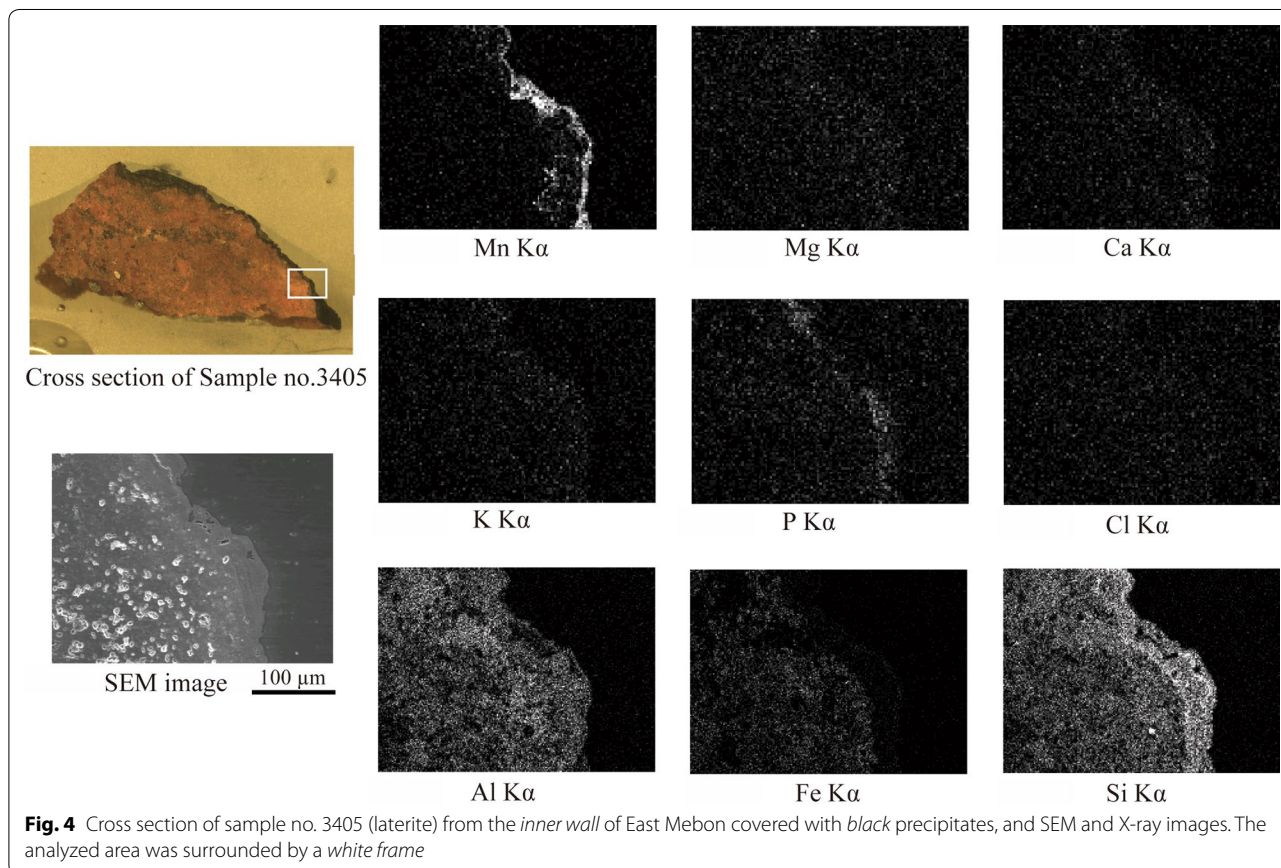
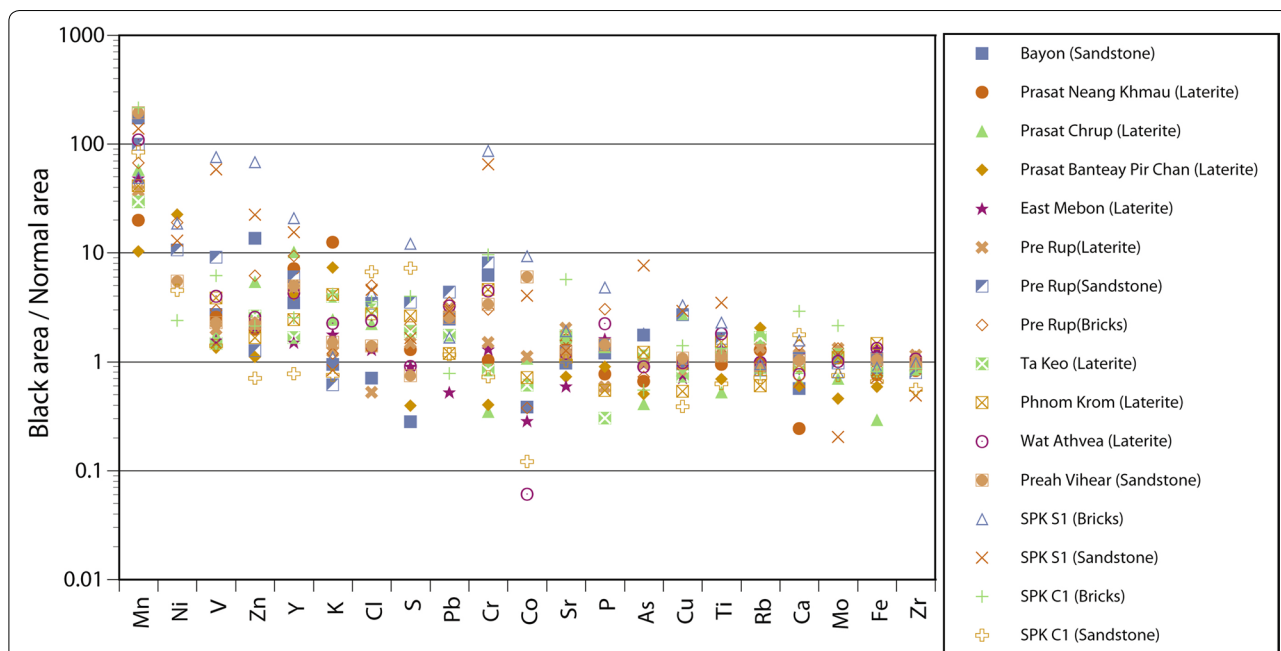


Table 3 SEM-EDX results for the black materials on the surface of the construction materials used in the Khmer temples

Temple	Sample no.	Mn ± s.d. (%)	Fe ± s.d. (%)	Na ± s.d. (%)	Mg ± s.d. (%)	Al ± s.d. (%)	Si ± s.d. (%)	K ± s.d. (%)	Ca ± s.d. (%)	Ti ± s.d. (%)	P ± s.d. (%)	S ± s.d. (%)	Cl ± s.d. (%)	
Bayon	3401	Blackened area	28.55 ± 15.73	10.59 ± 7.74	0.52 ± 0.47	5.71 ± 4.21	6.41 ± 4.02	22.64 ± 14.48	1.42 ± 3.23	1.67 ± 0.92	-	-	-	0.83 ± 0.48
		Sandstone Ratio	0.37 ± 0.18	5.22 ± 1.26	3.55 ± 1.19	2.60 ± 0.43	8.67 ± 2.13	39.08 ± 4.96	2.41 ± 1.24	1.67 ± 0.37	0.37 ± 0.14	-	-	-
East Mebon	3405	Blackened area	21.67 ± 5.91	2.76 ± 0.91	0.24 ± 0.09	-	10.59 ± 3.41	29.26 ± 2.78	0.88 ± 0.12	0.57 ± 0.22	1.03 ± 0.52	0.30 ± 0.84	0.16 ± 0.41	0.52 ± 0.30
		Laterite Ratio	0.18 ± 0.13	28.87 ± 2.89	0.09 ± 0.05	-	16.24 ± 0.46	20.40 ± 0.90	0.05 ± 0.09	0.09 ± 0.12	0.97 ± 0.23	0.59 ± 0.25	0.32 ± 0.19	0.12 ± 0.15
Pre Rup	3406	Blackened area	6.81 ± 2.66	2.29 ± 2.63	0.11 ± 0.04	0.21 ± 0.05	4.20 ± 2.29	33.84 ± 4.41	0.34 ± 0.06	0.28 ± 0.03	0.19 ± 0.25	0.05 ± 0.12	0.27 ± 0.28	0.05 ± 0.12
		Laterite Ratio	0.22 ± 0.11	29.80 ± 2.07	0.14 ± 0.03	-	10.63 ± 0.75	15.00 ± 1.89	-	-	0.42 ± 0.05	0.02 ± 0.05	0.02 ± 0.04	0.06 ± 0.07
Ta Keo	3407	Blackened area	12.36 ± 4.45	4.67 ± 3.47	2.80 ± 1.43	3.14 ± 2.30	7.48 ± 1.89	20.84 ± 6.57	1.82 ± 1.96	0.88 ± 0.44	-	0.88 ± 0.23	-	1.50 ± 0.72
		Sandstone Ratio	0.03 ± 0.04	1.80 ± 0.45	3.44 ± 1.06	1.21 ± 0.38	7.10 ± 1.31	32.90 ± 2.26	3.77 ± 2.13	0.40 ± 0.34	-	-	0.21 ± 0.00	0.88 ± 0.13
Phnom Krom	3408	Blackened area	18.29 ± 10.23	10.73 ± 5.68	0.18 ± 0.12	-	12.79 ± 3.00	14.17 ± 1.65	-	-	0.67 ± 0.38	1.00 ± 0.62	0.75 ± 0.60	-
		Laterite Ratio	0.56 ± 0.14	43.03 ± 0.96	0.14 ± 0.08	-	9.86 ± 0.66	8.51 ± 0.43	-	-	0.27 ± 0.23	-	-	-
Wat Athvea	3409	Blackened area	10.07 ± 3.63	4.28 ± 5.79	0.16 ± 0.09	-	19.28 ± 2.58	10.28 ± 3.57	-	-	-	2.39 ± 1.07	0.85 ± 0.39	0.53 ± 0.16
		Laterite Ratio	0.18 ± 0.17	21.33 ± 5.03	0.08 ± 0.05	-	6.77 ± 0.82	24.56 ± 4.80	-	-	0.40 ± 0.09	-	0.15 ± 0.13	-
Pr. Neang Khmau	3410	Blackened area	7.34 ± 1.26	3.30 ± 1.25	0.19 ± 0.15	-	9.42 ± 1.78	31.70 ± 3.05	0.63 ± 0.25	0.38 ± 0.20	0.48 ± 0.29	-	-	-
		Laterite Ratio	0.33 ± 0.27	3.05 ± 0.29	0.10 ± 0.04	-	12.42 ± 0.28	32.74 ± 0.27	0.68 ± 0.10	0.39 ± 0.21	0.37 ± 0.19	0.30 ± 0.00	-	-
Pr. Chrap	3402	Blackened area	4.91 ± 3.01	52.07 ± 8.03	0.27 ± 0.29	-	5.51 ± 2.09	3.22 ± 1.56	-	-	0.70 ± 0.42	0.87 ± 0.13	0.51 ± 0.23	0.89 ± 0.77
		Laterite Ratio	0.25 ± 0.18	54.92 ± 4.59	0.11 ± 0.05	-	4.16 ± 0.20	6.23 ± 1.70	-	-	0.65 ± 0.07	0.40 ± 0.04	0.03 ± 0.07	-
Pr. Chrap	3403	Blackened area	31.72 ± 13.36	6.36 ± 15.86	0.35 ± 0.29	0.41 ± 0.18	6.05 ± 1.78	9.21 ± 4.00	1.44 ± 0.61	0.45 ± 0.19	0.78 ± 0.40	0.46 ± 0.31	0.33 ± 0.18	0.40 ± 0.21
		Laterite Ratio	0.31 ± 0.10	51.78 ± 0.86	0.20 ± 0.15	-	6.09 ± 0.23	2.43 ± 0.24	0.05 ± 0.06	0.10 ± 0.13	0.89 ± 0.05	1.17 ± 0.10	0.05 ± 0.06	0.34 ± 0.10
			102.99	0.12	1.77	0.99	3.78	27.66	4.32	0.87	0.39	6.58	1.19	

Table 3 continued

Temple	Sample no.	Mn ± s.d. (%)	Fe ± s.d. (%)	Na ± s.d. (%)	Mg ± s.d. (%)	Al ± s.d. (%)	Si ± s.d. (%)	K ± s.d. (%)	Ca ± s.d. (%)	Ti ± s.d. (%)	P ± s.d. (%)	S ± s.d. (%)	Cl ± s.d. (%)
Pr. Banteay Pir	3404	10.85 ± 6.22		0.62 ± 0.69	-	11.05 ± 2.77	12.03 ± 4.81	0.92 ± 0.42	0.32 ± 0.04	1.30 ± 0.42	0.99 ± 0.31	-	0.53 ± 0.34
	Chan												
		1.03 ± 0.79	24.30 ± 12.48	0.67 ± 0.56	-	9.09 ± 1.70	8.64 ± 1.25	-	-	1.10 ± 0.44	0.96 ± 0.20	-	-
	Laterite												
		10.55	0.99	0.93	-	1.22	1.39	-	-	1.19	1.04	-	-
	Ratio												
Sambor Prei	3411	3.87 ± 2.93	1.50 ± 0.73	0.39 ± 0.18	0.81 ± 0.23	6.10 ± 1.51	33.27 ± 9.41	1.14 ± 0.24	0.71 ± 0.82	-	2.73 ± 2.04	1.59 ± 1.42	0.46 ± 0.27
	Kuk S1												
	area												
	tower	0.09 ± 0.06	0.37 ± 0.46	0.32 ± 0.12	-	2.46 ± 0.39	44.84 ± 1.11	0.67 ± 0.24	-	-	-	0.39 ± 0.21	0.24 ± 0.20
	Bricks												
		45.05	4.01	1.21	-	2.48	0.74	1.71	-	-	-	4.07	1.90
	Ratio												
3412	Blackened	8.71 ± 3.19	0.96 ± 3.24	2.95 ± 1.70	0.66 ± 1.28	3.98 ± 3.82	13.63 ± 11.33	1.18 ± 1.62	4.37 ± 2.71	-	5.62 ± 3.63	4.28 ± 1.05	-
	area												
	Sandstone	0.22 ± 0.10	2.46 ± 0.63	3.39 ± 0.93	0.93 ± 0.22	6.88 ± 1.55	36.51 ± 2.13	2.97 ± 1.08	0.47 ± 0.28	-	-	-	0.33 ± 0.00
	Ratio	38.88	0.39	0.87	0.71	0.58	0.37	0.40	9.26	-	-	-	-
Sambor Prei	3413	48.41 ± 1.69	-	0.30 ± 0.19	4.18 ± 0.57	0.54 ± 0.50	3.84 ± 1.30	1.90 ± 0.16	2.84 ± 0.23	-	0.39 ± 0.14	-	0.22 ± 0.20
	Kuk C1												
	area												
	tower	0.09 ± 0.07	1.19 ± 0.22	0.30 ± 0.09	0.13 ± 0.11	3.66 ± 0.81	45.76 ± 2.14	1.26 ± 0.17	0.07 ± 0.14	0.43 ± 0.06	-	0.49 ± 0.00	0.36 ± 0.21
	Bricks												
		562.93	-	0.98	31.18	0.15	0.08	1.50	40.54	-	-	-	0.61
	Ratio												
3414	Blackened	16.12 ± 6.89	2.05 ± 3.80	0.74 ± 1.49	6.23 ± 1.78	3.06 ± 2.14	20.60 ± 8.45	1.68 ± 1.54	3.17 ± 4.48	1.49 ± 4.52	0.38 ± 0.20	-	0.51 ± 0.20
	area												
	Sandstone	1.06 ± 0.44	1.55 ± 1.90	3.72 ± 3.52	1.21 ± 0.47	7.34 ± 3.96	36.99 ± 6.09	1.68 ± 1.11	1.59 ± 2.02	0.20 ± 0.25	-	-	-
	Ratio	15.21	1.32	0.20	5.16	0.42	0.56	1.00	2.00	7.46	-	-	-

Each analysis was conducted on a polished cross section of the sample

in the black materials under the detection limit of the SEM-EDX.

The concentration ratio of each element in the black area to that in the non-black area is shown in Fig. 5. This figure shows that Mn was considerably concentrated in the black area. In addition, slightly higher levels of Mg, Ca, and K were found in the black areas than those in the non-black areas (Fig. 4).

XRD analysis

The results of the XRD analysis are shown in Table 4.

Quartz, plagioclase, goethite and kaolinite were detected in many of the samples, and could be attributed to the construction materials (sandstone, laterite and bricks). Brushite ($\text{CaHPO}_4 \cdot 2\text{H}_2\text{O}$) was found in the samples from the Sambor Prei Kuk monuments, and could be attributed to bat guano [12, 13]. Typical peaks for manganese minerals were not detected, which suggest the manganese precipitates exist as amorphous materials or nanoscale materials with low levels of crystallization. X-ray peaks corresponding to birnessite ($(\text{Na}, \text{Ca}, \text{K})_x(\text{Mn}^{4+}, \text{Mn}^{3+})_2\text{O}_4 \cdot 1.5\text{H}_2\text{O}$) and 10 Å manganese oxide minerals were detected in several samples (Fig. 6). The 10 Å manganese oxide minerals could be buserite ($\text{Na}_4\text{Mn}_{14}\text{O}_{27} \cdot 21\text{H}_2\text{O}$) and/or todorokite ($(\text{Na}, \text{Ca}, \text{K})_x(\text{Mn}^{4+}, \text{Mn}^{3+})_6\text{O}_{12} \cdot 3-4.5\text{H}_2\text{O}$).

It has been shown that buserite will convert to birnessite with dehydration on heating at 105 °C [7, 14]. Therefore, the black precipitates that showed X-ray peaks corresponding to 10 Å manganese oxide minerals were heated at 105 °C in an oven for 24 h to identify the mineral. After heating, no change in the X-ray peaks was observed. Consequently, the mineral was identified as todorokite. These findings are consistent with studies that have shown birnessite, todorokite, buserite, and vernadite are the major constituents of manganese nodules and crusts on the sea floor [15–17]. Birnessite is also the main manganese mineral found in desert varnish [5].

FE-SEM analysis

Stacks of hexagonal plates ranging in size from 100 to 200 nm in diameter were common in the samples of the manganese oxide precipitates (Fig. 7). In addition, some of the precipitates showed rod-shaped structures with lengths between 100 and 300 nm. The images for several of the samples showed areas with the rod-shaped structures incorporated into and forming the hexagonal plates. The rod-shaped structures suggest that the precipitation of manganese oxides may have been initiated by the activity of manganese oxidizing microbes. Manganese oxidizing bacteria have also been found in manganese

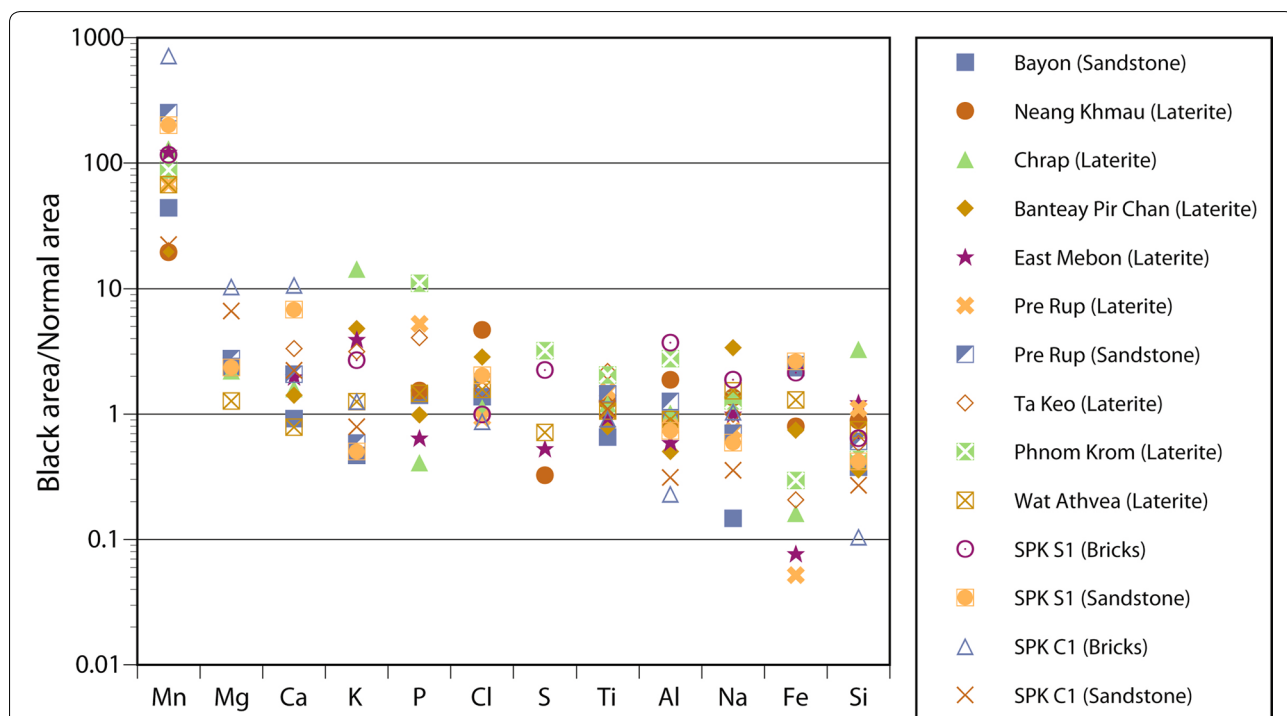
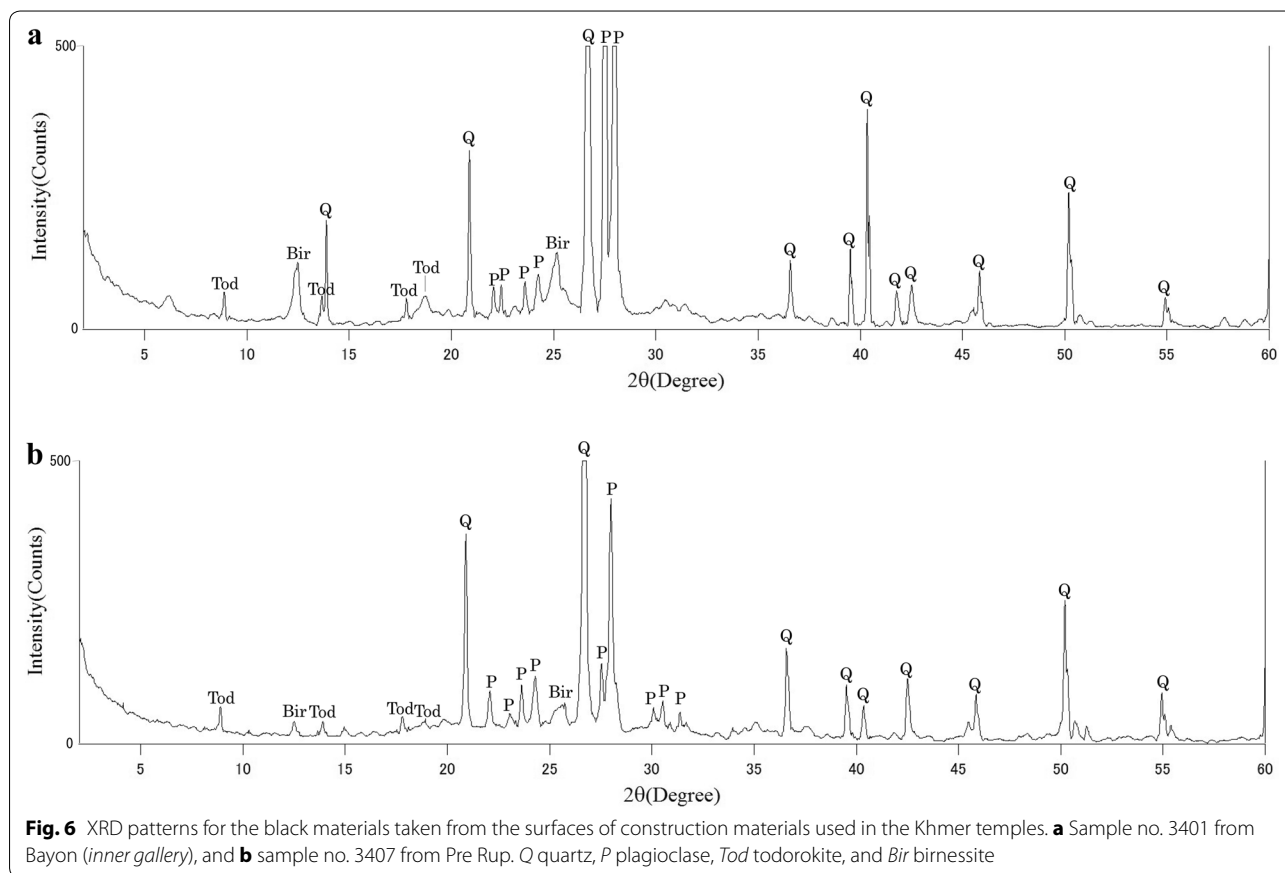


Fig. 5 SEM-EDX results expressed as concentration ratios for elements in the black areas to those in the non-black areas on the surfaces of construction materials used in the Khmer temples

Table 4 XRD results for the black materials on the surface of the construction materials used in the Khmer temples

Temple	Sample no.	Base material	Quartz	Plagioclase	Goethite	Kaolinite	Birnessite	Todorokite	Brushite
Bayon	3401	Sandstone	○	○			○	○	
Prasat Neang Khmau	3402	Laterite	○		○			○	
Prasat Chrap	3403	Laterite	○						
Prasat Banteay Pir Chan	3404	Laterite			○				
East Mebon	3405	Laterite	○			○			
Pre Rup	3406	Laterite	○		○	○			
Pre Rup	3407	Sandstone	○	○			○	○	
Ta Keo	3408	Laterite	○		○	○			
Phnom Krom	3409	Laterite	○		○	○			
Wat Athvea	3410	Laterite	○		○	○			
Sambor Prei Kuk: Tower S1	3411	Bricks	○						
Sambor Prei Kuk: Tower S1	3412	Sandstone	○	○			○	○	○
Sambor Prei Kuk: Tower C1	3413	Bricks	○						
Sambor Prei Kuk: Tower C1	3414	Sandstone	○	○			○	○	○



nodules and crusts on the sea floor and in desert varnish [6, 18, 19]. In addition, Hariya and Kanari [20] reported that bacteria caused precipitation of manganese oxides in a spring.

Preliminary experiments on removal of manganese oxide precipitates

The solubility of tetravalent manganese ion is low, but that of divalent manganese ion is high. Therefore the

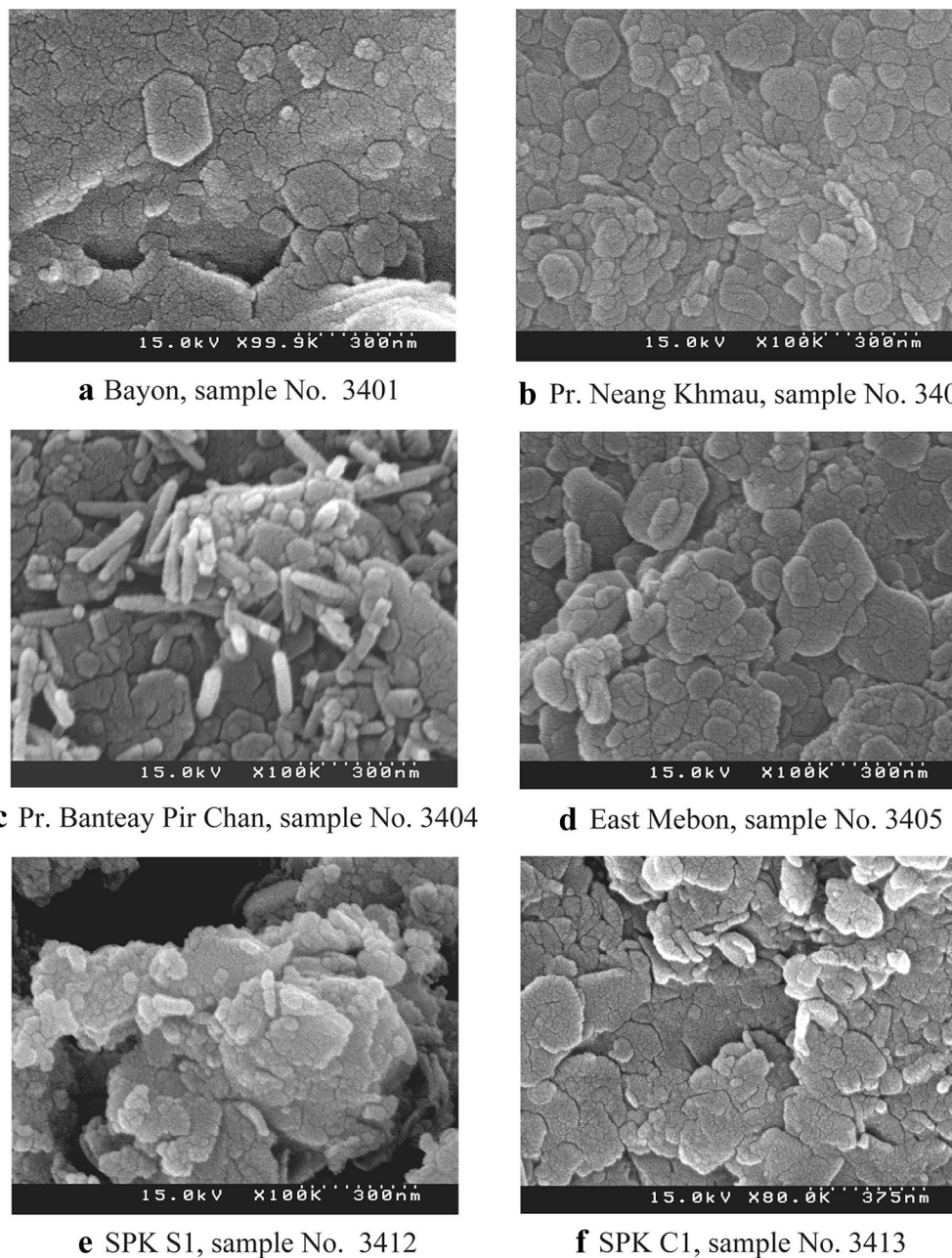


Fig. 7 FE-SEM images of the manganese oxide precipitates on the surfaces of construction materials used in the Khmer temples. **a** Sample no. 3401 from Bayon, **b** sample no. 3402 from Neang Khmau, **c** sample no. 3404 from Banteay Pir Chan, **d** sample no. 3405 from East Mebon, **e** sample no. 3412 from tower S1 at the Sambor Prei Kuk monuments, and **f** sample no. 3413 from the tower C1 at the Sambor Prei Kuk monuments

reduction of manganese may be the best method to remove the manganese oxide precipitates on the surface of construction materials.

In this context, we carried out the preliminary experiment on removal of manganese oxide precipitates using an oxalic acid solution with a concentration of 0.1 mol/l as a reducing agent. The laterite sample from

Prasat Chrap (sample no. 3615), covered with manganese oxide precipitates was immersed in the oxalic acid solution for 0, 1, 3 and 5 h. The photographs of the sample before and after the experiments are shown in Fig. 8. Almost all manganese oxides disappeared within 3 h after the immersion into the oxalic acid solution. No visible change of laterite was observed. The same result was

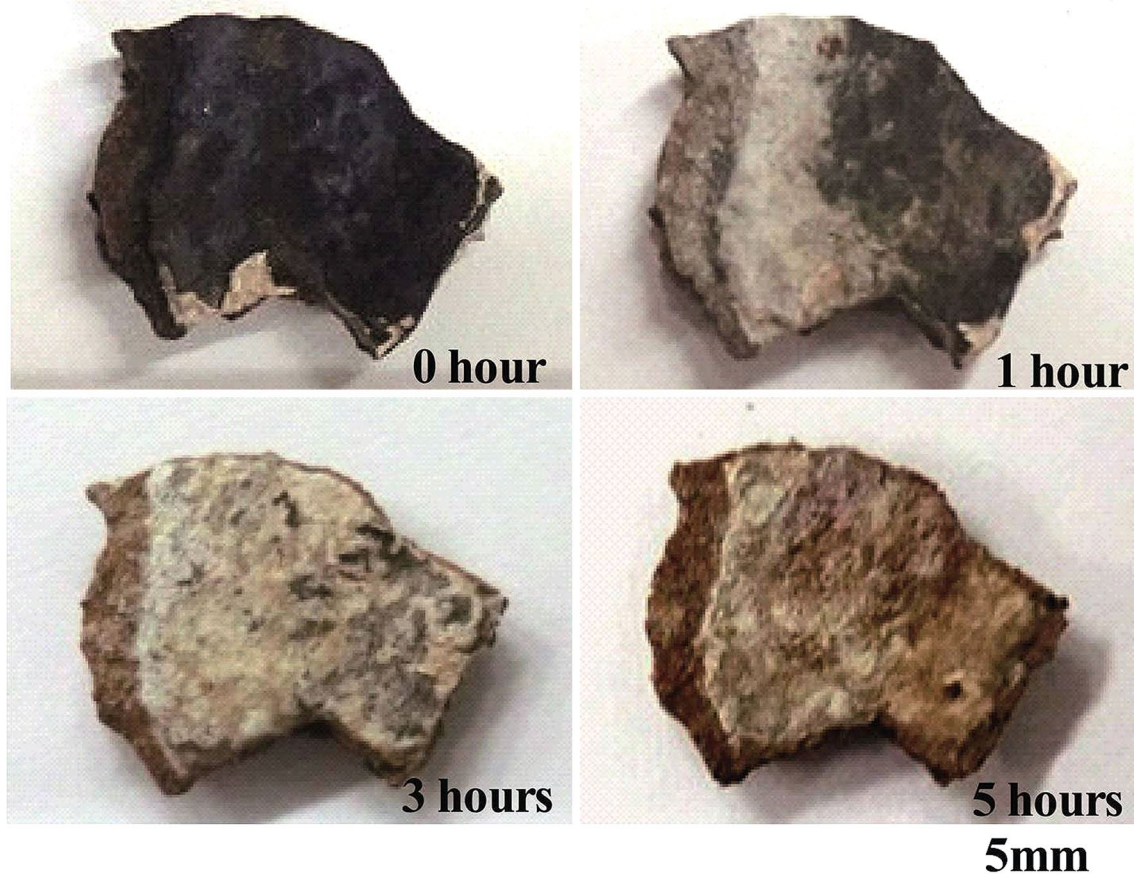


Fig. 8 Photographs of the laterite sample from the *inner wall* of Prasat Chrap (sample no. 3615) covered with manganese oxide precipitates after the experiment of immersion into the oxalic acid solution of a concentration of 0.1 mol/l for 0, 1, 3 and 5 h, respectively

obtained for sandstone covered with manganese oxide precipitates. Therefore the reduction using a reducing agent such as an oxalic acid is a useful method to removal of manganese oxide precipitates.

Conclusions

Blackening caused by something other than the growth of blue-green algae is frequently observed on the surface of construction materials used in the Khmer temples in Cambodia. The results of this study showed that the black areas are caused by precipitation of manganese oxides. In addition to Mn, the precipitates contain small amounts of Ni, V, Zn, Y, K, Cl, S, Pb, and Cr. The manganese oxides mainly exist as an amorphous phase, but some are present as birnessite and todorokite. The precipitates are mostly present as hexagonal plates ranging in size from 100 to 300 nm, but some are rod-shaped. This suggests that precipitation of manganese oxides may have been initiated by the activity of manganese oxidizing microbes.

The manganese oxide precipitates could be easily removed using a reducing agent such as an oxalic acid solution.

Authors' contributions

EU designed this study. All the authors carried out the field investigation. RW and SO conducted the laboratory work. All the authors interpreted data. EU drafted the manuscript. All authors read and approved the final manuscript.

Author details

¹ Department of Resources and Environmental Engineering, Waseda University, Ohkubo 3-4-1, Shinjuku-ku, Tokyo 169-8555, Japan. ² Department of Earth and Planetary Science, The University of Tokyo, Hongo 7-3-1, Bunkyo-ku, Tokyo 113-0033, Japan.

Acknowledgements

This research was conducted with permission from Authority for Protection and Management of Angkor and the Region of Siem Reap (APSARA National Authority), and was supported in part by a Grant-in-Aid for Scientific Research of the Japan Society for the Promotion of Science (Grant No. 23401001: E. Uchida, No. 25257303: T. Matsui of the University of Tsukuba). We would like to express our gratitude to all the members of JASA for their kind help during the research.

Competing interests

The authors declare that they have no competing interests.

Received: 17 December 2015 Accepted: 10 May 2016

Published online: 27 June 2016

References

- Uchida E, Ogawa Y, Nakagawa T. The stone materials of the Angkor monuments, Cambodia. The magnetic susceptibility and the orientation of the bedding plane of the sandstone. *J Min Pet Econ Geol*. 1998;93:411–26.
- Uchida E, Maeda N, Nakagawa T. The laterites of the Angkor monuments, Cambodia. The grouping of the monuments on the basis of the laterites. *J Min Pet Econ Geol*. 1999;94:162–75.
- Arai H, Yamagishi T. Conservation science. In: Japanese Government Team for Safeguarding Angkor, editor. Annual report on the technical survey of Angkor monument 1998, Japan International Cooperation Center, Japan, 1998. p. 393–406.
- Uchida E, Watanabe R. Blackening of the surfaces of Mesopotamian clay tablets due to manganese precipitation. *Archaeol Discov*. 2014;2:107–16.
- Potter RM, Rossman GR. Desert varnish: the importance of clay minerals. *Science*. 1977;196:1446–8.
- Potter RM, Rossman GR. The manganese- and iron-oxide mineralogy of desert varnish. *Chem Geol*. 1979;25:79–94.
- Dorn RI, Oberlander TM. Microbial origin of desert varnish. *Science*. 1981;213:1245–7.
- Imai N, Terashima S, Itoh S, Ando A. 1994 compilation values for GSJ reference samples, "Igneous rock series". *Geochem J*. 1995;29:91–5.
- Uchida E, Tsuda K, Shimoda I. Construction sequence of the Koh Ker monuments in Cambodia deduced from the chemical composition and magnetic susceptibility of its laterites. *Herit Sci*. 2014;2:1–11.
- Hein JR, Koschinsky A, Halliday AN. Global occurrence of tellurium-rich ferromanganese crusts and a model for the enrichment of tellurium. *Geochim Cosmochim Acta*. 2003;67:1117–27.
- Dorn RI, Krinsley DH, Liu T, Anderson S, Clark J, Cahill TA, Gill TE. Manganese-rich rock varnish does occur in Antarctica. *Chem Geol*. 1992;99:289–98.
- Hosono T, Uchida E, Suda C, Ueno A, Nakagawa T. Salt weathering of sandstone at the Angkor monuments, Cambodia: identification of the origins of salts using sulfur and strontium isotopes. *J Archaeol Sci*. 2006;33:1541–51.
- Uchida E, Ogawa Y, Maeda N, Nakagawa T. Deterioration of stone materials in the Angkor monuments, Cambodia. *Eng Geol*. 1999;55:101–12.
- Usui A, Mellin TA, Nohara M, Yuasa M. Structural stability of marine 10\AA manganates from the Ogasawara (Bonin) arc: implication for low-temperature hydrothermal activity. *Mar Geol*. 1989;86:41–56.
- Giovanoli R, Feitknecht W, Fischer F. Über oxidhydroxide des vierwertigen Mangans mit Schichtengitter, 3. Mitteilung: reduktion von Mangan (III)-manganat (IV) mit Zimtalkohol. *Helv Chim Acta*. 1971;54:1112–24.
- Burns RG, Burns VM, Stockman HW. A review of the todorokite - buserite problem: implications to the mineralogy of marine manganese nodules. *Am Mineral*. 1983;68:972–80.
- Usui A, Someya M. Distribution and composition of marine hydrogenetic and hydrothermal manganese deposits in the northwest Pacific. In: Nicholson K, Hein JR, Böhn B, Dasgupta S, editors. Manganese mineralization: geochemistry and mineralogy of terrestrial and marine deposits. London: Geological Society of London Special Publication No. 119; 1997. p. 177–98.
- Wang W, Müller WEG. Marine biominerals: perspectives and challenges for polymetallic nodules and crusts. *Trends Biotechnol*. 2009;27:375–83.
- Wang X, Zeng L, Wiens M, Schloßmacher U, Jochum KP, Schröder HC, Müller WEG. Evidence for a biogenic, microorganismal origin of rock varnish from the Gangdese Belt of Tibet. *Micron*. 2011;42:401–11.
- Hariya Y, Kikuchi T. Precipitation of manganese by bacteria in mineral springs. *Nature*. 1964;202:416–7.

Submit your manuscript to a SpringerOpen[®] journal and benefit from:

- Convenient online submission
- Rigorous peer review
- Immediate publication on acceptance
- Open access: articles freely available online
- High visibility within the field
- Retaining the copyright to your article

Submit your next manuscript at ► springeropen.com
